A novel method to calibrate DOI function of a PET detector with a dual-ended-scintillator readout

Yiping Shao[a)]
Department of Imaging Physics, University of Texas M.D. Anderson Cancer Center, 1515 Holcombe Boulevard, Unit 600, Houston, Texas 77030

Rutao Yao
Department of Nuclear Medicine, State University of New York at Buffalo, 105 Parker Hall, 3435 Main Street, Buffalo, New York 14214

Tianyu Ma
Department of Nuclear Medicine, State University of New York at Buffalo, 105 Parker Hall, 3435 Main Street, Buffalo, New York 14214 and Department of Engineering Physics, Tsinghua University, Beijing, 100084, People's Republic of China

(Received 5 May 2008; revised 26 September 2008; accepted for publication 20 October 2008; published 20 November 2008)

The detection of depth-of-interaction (DOI) is a critical detector capability to improve the PET spatial resolution uniformity across the field-of-view and will significantly enhance, in particular, small bore system performance for brain, breast, and small animal imaging. One promising technique of DOI detection is to use *dual-ended-scintillator* readout that uses two photon sensors to detect scintillation light from both ends of a scintillator array and estimate DOI based on the ratio of signals (similar to Anger logic). This approach needs a careful DOI function calibration to establish accurate relationship between DOI and signal ratios, and to recalibrate if the detection condition is shifted due to the drift of sensor gain, bias variations, or degraded optical coupling, etc. However, the current calibration method that uses coincident events to locate interaction positions inside a single scintillator crystal has severe drawbacks, such as complicated setup, long and repetitive measurements, and being prone to errors from various possible misalignments among the source and detector components. This method is also not practically suitable to calibrate multiple DOI functions of a crystal array. To solve these problems, a new method has been developed that requires only a uniform flood source to irradiate a crystal array without the need to locate the interaction positions, and calculates DOI functions based solely on the uniform probability distribution of interactions over DOI positions without knowledge or assumption of detector responses. Simulation and experiment have been studied to validate the new method, and the results show that the new method, with a simple setup and one single measurement, can provide consistent and accurate DOI functions for the entire array of multiple scintillator crystals. This will enable an accurate, simple, and practical DOI function calibration for the PET detectors based on the design of dual-ended-scintillator readout. In addition, the new method can be generally applied to calibrating other types of detectors that use the similar dual-ended readout to acquire the radiation interaction position.
[DOI: 10.1118/1.3021118]

Key words: depth of interaction, detector calibration, positron emission tomography

I. INTRODUCTION

It is well known that the PET performance can be significantly improved if its detectors can measure depth-of-interaction (DOI), since this will reduce the parallex error due to the crystal penetration by energetic 511 keV gamma photons, minimize the spatial resolution loss (mainly along the radial direction) at the off-center region, and improve the spatial resolution uniformity across the field-of-view (FOV).[1] This DOI measurement capability is particularly important for a system with small bore configuration since it leads to severe parallex errors.[2,3] One common remedy to this problem is to use short crystals (~10 mm); however, this significantly reduces system sensitivity.[4]

There are several different detector designs to measure DOI, with different performance trade-offs.[5–17] One design that has been well studied is to measure DOI by detecting signals from both ends of a crystal with compact photon sensors such as avalanche photo diodes (APDs).[8,14,18,19] For simplicity, this detector design is defined as "dual-ended-scintillator readout" in this study, or simply the DES readout. Since the ratio of the signals is related to the interaction position along the crystal long axis, DOI can be calculated based on a predetermined function between the signal ratio and DOI, which in principle is to apply "Anger logic" to calculate the one-dimensional interaction position. This function, defined as DOI function in this study, has to be experimentally determined for each and every crystal inside a crys-

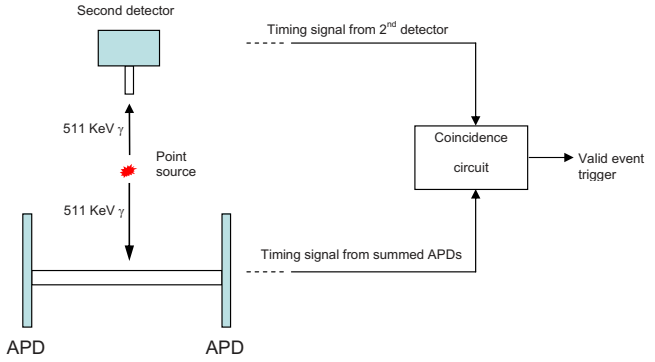

FIG. 1. Schematic drawing of the primary current method to measure DOI function. A primary scintillator crystal is read out from its two ends by two photon sensors (e.g., avalanche photodiode). A point source and a second detector are used to electronically collimate the interaction positions (DOI). The ratio of measured signals from the first detector at different interaction positions is used to calculate DOI function.

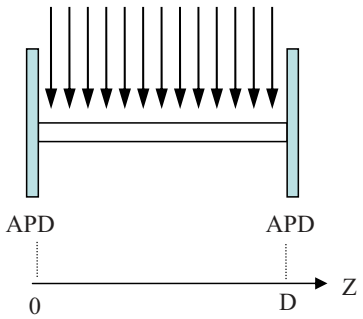

FIG. 2. Schematic drawing of the new method. There is no second detector and coincidence processing. A parallel beam of gamma rays irradiates the crystal to generate a uniform distribution of interaction positions over the crystal length *D*.

tal array. The required accuracy in determining such DOI function varies with detector and system designs, and usually is ~5.0 mm for the system with detector ring diameter at ~10.0 cm or larger.[14,18,19] Since DOI function may drift over time due to various factors such as the gain drift of photon sensors, variations of operating conditions (e.g., voltage bias and temperature), and the change of optical coupling between the scintillators and photon sensors, etc., DOI function is expected to be recalibrated periodically during the operation of a practical PET system.

Several methods have been studied to measure DOI function of either a single crystal or an array of crystals with one-to-one coupling between a crystal and a photon sensor.[20–22] However, as will be illustrated in the following section, there are severe drawbacks or limitations associated with these current methods which make them difficult to be used for a practical PET detector.

In this study, we have developed and validated a new calibration method to measure DOI function with the DES readout. The method was investigated with both Monte Carlo simulations and experimental measurements and compared with the current method. The results have shown that the new method can accurately measure DOI function without the technical problems existing in the current methods. The new method is expected to provide a good solution to the measurement and recalibration of DOI functions for PET detectors that use the DES readout with a one-to-one coupling between a crystal and a photon sensor.

It is important to point out that both the current method and new method are applied for a detector with an independent readout of one-to-one coupling between a crystal and a photon sensor. In practice, many PET detectors are designed with sharing of scintillation photons and/or electric signals among different crystals in order to reduce the complexity of readout. However, one performance drawback of these detectors is that the accuracy to determine the interaction crystal and DOI with DES readout will be reduced owing to the crystal cross-talk. The level of this inaccuracy is dependent on the specific characteristics and amount of the crystal cross-talk and needs to be addressed individually. The new method calibrates DOI function with independent crystal readout and will provide a basis to further investigate the impact from crystal cross-talk.

II. METHOD

II.A. Current methods of a DOI function measurement

The primary current method to determine DOI function is to use a coincidence method to locate the interaction position for measuring the relationship between DOI and the signal ratio.[8] As schematically shown in Fig. 1, a point source is placed between the primary detector (with its DOI function to be determined) and a second small dimension detector. Coincidence events between the two detectors are acquired to electronically collimate the interaction (DOI) position along the long axis of the primary detector. The signal ratios between the two photon sensors at the two ends of the primary detector are calculated to establish the relationship between this particular DOI position and its corresponding values of signal ratios. In order to measure DOI function, which is the relationship between DOI positions and the signal ratios over the entire crystal length, the point source and the second detector have to be moved along the long axis of the primary detector for taking multiple measurements at different DOI positions.

There are several drawbacks associated with this method: It requires a complicated experimental setup of two detectors and coincidence processing; it measures multiple DOI positions over the crystal which leads to lengthy acquisition time and potential detector performance variations; and it is prone to measurement errors due to potential misalignment among the detectors and the source, etc. More importantly, it is difficult if not impossible for this method to measure DOI functions of all crystals inside an array, since inevitable intercrystal scatters can severely blur DOI localization. Therefore, it is very challenging to use this method to calibrate a practical PET detector that consists of an array of crystals.

There are two other methods that have been developed to measure DOI function of an array of crystals, which are briefly summarized below:

(1) The second method is based on irradiating the crystals

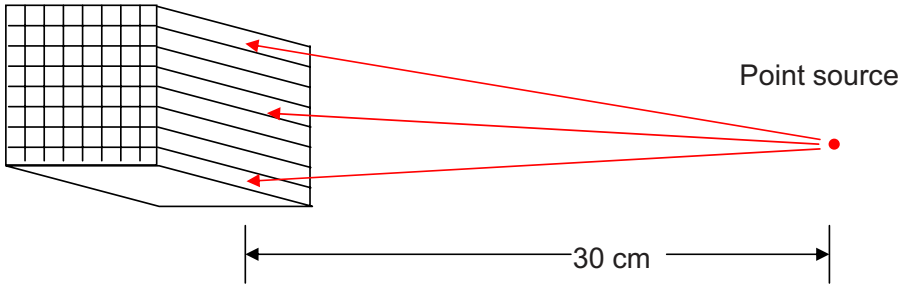

(a)

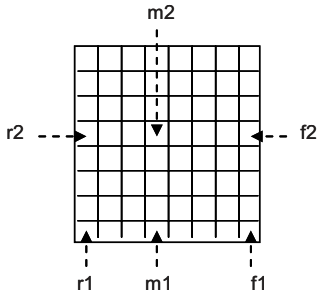

(b)

FIG. 3. Schematic drawing of the crystal array for the Monte Carlo simulation studies. (a) An 8×8 array of $2\times2\times20$ mm^3 LSO crystals were approximately uniformly irradiated along the crystal long axial direction by a point source which was placed 30 cm away from the side of the crystal array. (b) Six representative crystals inside the crystal array: f_1 and f_2 are in the front row, m_1 and m_2 in the middle row, r_1 and r_2 in the rear row.

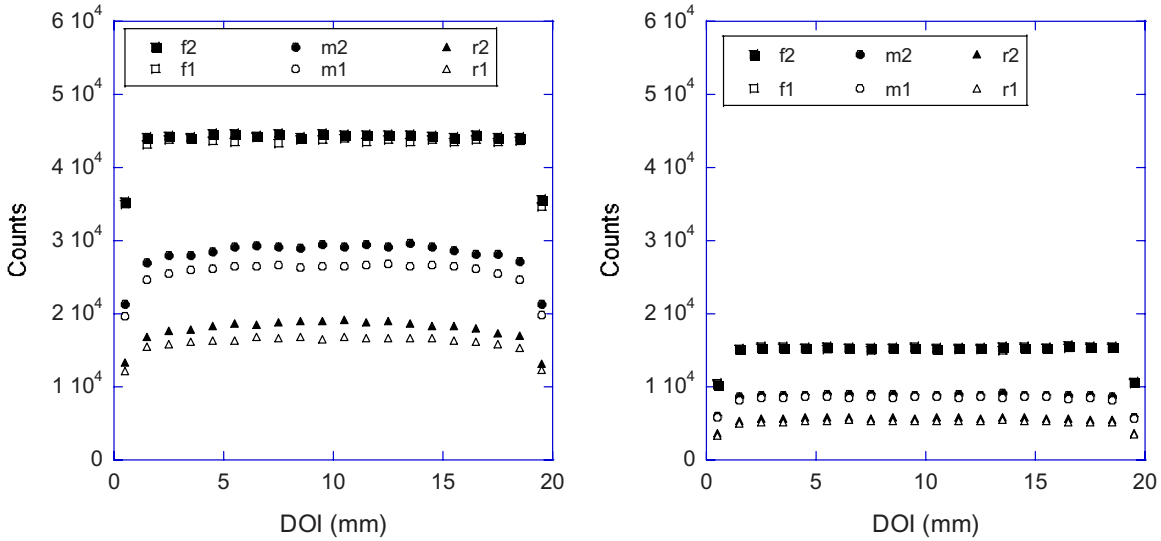

FIG. 4. Distribution of DOI positions with different front and back crystals, calculated with energy thresholds at 200–650 keV (left) and 350–650 keV (right). While the uniformities of distributions calculated from front crystals are always excellent for both energy thresholds, the uniformity of the back crystals are slightly deteriorated with the lower energy threshold, with a less than 10% maximum change at the central region. The counts at the very edges of DOI are always significantly lower than at the other DOI positions, which is mainly due to the edge effect of gamma ray escaping. A slight difference in total counts for crystals within the same rows (e.g., between the m_1 and m_2 crystals) was due to the imperfect uniform source and scatters with different path length. However, the shapes of DOI distributions for crystals within the same rows are the same, indicating that the consistent DOI functions among these crystals can be measured under these practical application conditions.

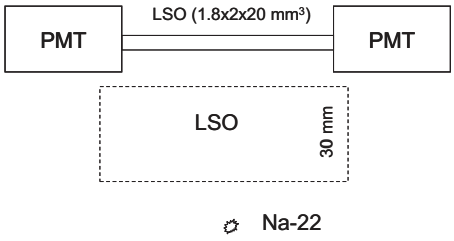

FIG. 5. Schematic drawing of experimental setup for DOI measurement with the new method. A $1.8\times2\times20$ mm^3 LSO crystal was wrapped with white Teflon tape and read out by two single-channel PMTs (Hamamatsu R7400-02). A Na-22 point source was placed ~213.0 mm away from the crystal. For measuring DOI function of a back crystal, a bulk of LSO with ~30.0 mm thickness was placed between the crystal to be detected and the source to mimic the attenuation and scatter effects that will pose to back crystals. The detector operating conditions were kept the same during the measurements.

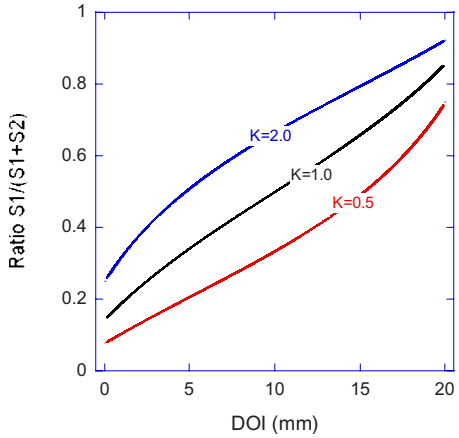

FIG. 6. Signal ratio as a function of DOI position with simulated interactions, with $K=0.5$, 1.0, and 2.0. A signal amplitude was calculated based on the light collection function defined in Eq. (8) and (9), without any dispersion. These functions are considered as the original DOI functions. All these calculations were based on one front crystal, indicated as f_2 in Fig. 3.

from the imaging object side of the detector array, with the gamma ray beam parallel to the long axis of the crystals.[21] Since the distribution of interaction probability along this direction should in theory be exponential, the density of detected DOI positions is also expected to be exponential if both photon sensors have the same gain. Assuming that the detected signal ratios are linearly dependent on DOI positions, one can extract the information about DOI function by fitting the energy spectra of the two detectors with corresponding expected exponential functions. The drawbacks of the method are that it is challenging to precisely align the long axis of crystals with the beam, and even a small misalignment with small deviation angle could lead to augmented errors; intercrystal scatter can significantly alter the expected exponential distribution of DOI positions; and the accuracy of the method is strongly dependent on the linearity of the detected signals with DOI positions, while in reality this relationship is usually complicated and can be very different from a linear function.[18,19,23]

(2) The third method uses LSO's natural background radiation as a uniform source across the long axis of the crystals.[22] The method also assumes a linear relationship between the detected signal ratios and DOI positions. In addition, it also requires symmetric performance between the two photon sensors, which has to be achieved by adjusting their gains. By fitting and linearly dividing the distribution of signal ratios detected from the photon sensors, one can estimate DOI function. Similar to the second method, the accuracy of the third method will strongly depend on if there is a good linear relationship between the detected signal ratios and DOI positions, as well as equal signal gains of the two detectors. Besides, it requires estimating the rising and falling edges of the distribution of signal ratios empirically from an additional prior detector calibration, which is cumbersome and can lead to more errors. If the gains of the photon detector shift differently, the method is unable to recalibrate DOI function.

Overall, the second and third methods are strongly dependent on several assumptions and approximations that may be valid for certain particular detectors and operations. However, they do not provide a general calibration method that can be used for different detector performances at various different detector operation conditions.

II.B. New method of a DOI function measurement

The concept of the new method is shown in Fig. 2: The detector is uniformly irradiated from the side so that interactions are uniformly distributed over the crystal depth. The probability of the interaction, $P(z)$, will be constantly distributed over the axis z. Since the total probability of interaction equals to 1, we have

$$\int_0^D P(z)dz = P(z)\int_0^D dz = P(z)^*D = 1, \tag{1}$$

where D is the total length of the crystal and z is the depth or DOI position. From Eq. (1), we have $P(z)=1/D$. The ratio of signals detected from two photon sensors at the two scintillator ends can be defined as

$$R = s_1/(s_1+s_2), \tag{2}$$

where s_1 and s_2 are the signal amplitudes from the two individual photon sensors. The collected histogram of R is denoted as $H(R)$, which is a measured distribution of R. A probability density function (PDF) can be calculated from $H(R)$ as

$$\mathrm{PDF}(R) = H(R) \Big/ \int_0^1 H(R)dR. \tag{3}$$

PDF(R) is a measured probability corresponding to an interaction at a DOI position z that will produce the signal ratio equal to R. If there is no signal dispersion from the detector response, then there is a one-to-one relationship between

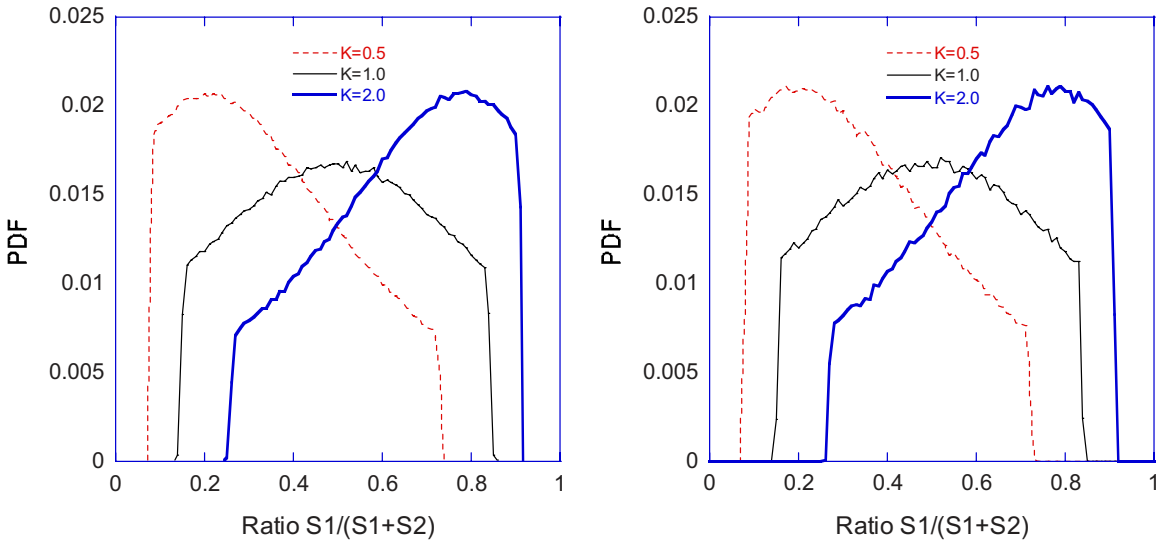

FIG. 7. Calculated PDFs without signal dispersion, with energy thresholds at 200–650 keV (left) and 350–650 keV (right).

DOI position z and the signal ratio R, and so will be the probabilities of $P(z)$ and PDF(R). If there is signal dispersion from the detector response, this one-to-one relationship will be between DOI position z and the mean of corresponding signal ratios. Therefore, we have a general formula

$$\int_0^Z P(z)dz = \int_0^R \mathrm{PDF}(R)dR. \tag{4}$$

In general, Eq. (4) is valid for any distribution of interaction positions. For a uniform distribution of interaction positions with $P(z)=1/D$, the left hand side of Eq. (4) equals to z/D. If we define $z'=z/D$ as a normalized depth (ranging from 0.0 to 1.0), we have

$$z = D^* \int_0^R \mathrm{PDF}(R)dR, \tag{5}$$

or

$$z' = \int_0^R \mathrm{PDF}(R)dR. \tag{6}$$

The left hand side of Eq. (5) and (6) is the exact DOI function to be determined, and the right hand side is a function of R that can be easily calculated from the measurement. This new method immediately provides several important advantages over the current method:

(1) A single non-coincident data acquisition is good enough to complete the measurement, which will vastly simplify complicated setup of the first method and eliminate the need of multiple measurements at different locations that is associated with lengthy acquisition time and source of errors.
(2) The new method can be straightforwardly applied to all crystals inside a detector array, since the distribution of interaction positions with intercrystal scatters is in prin-

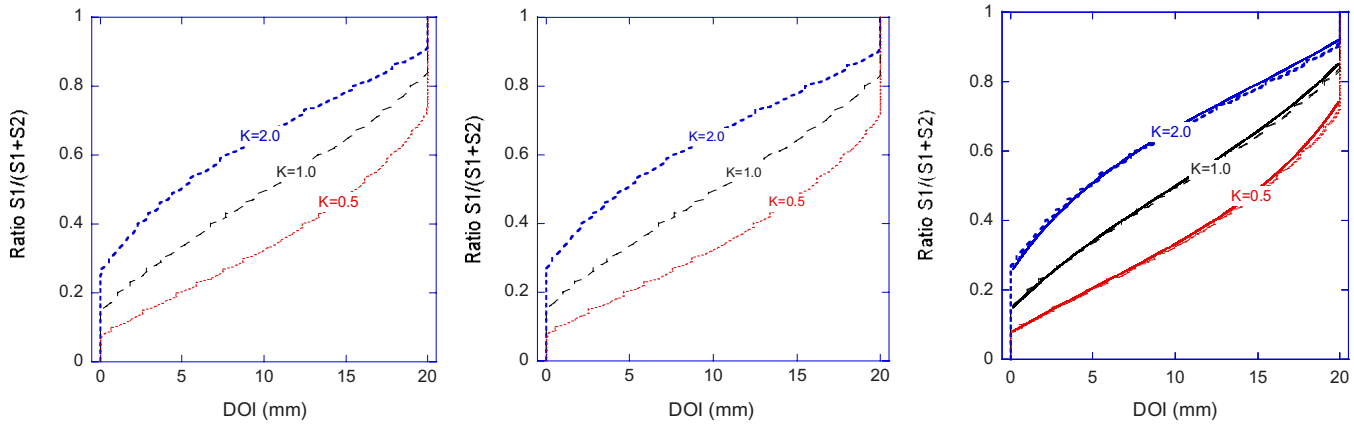

FIG. 8. Calculated DOI functions without signal dispersion, with energy thresholds at 200–650 keV (left) and 350–650 keV (middle). Both DOI functions were superimposed together with the original DOI functions (right).

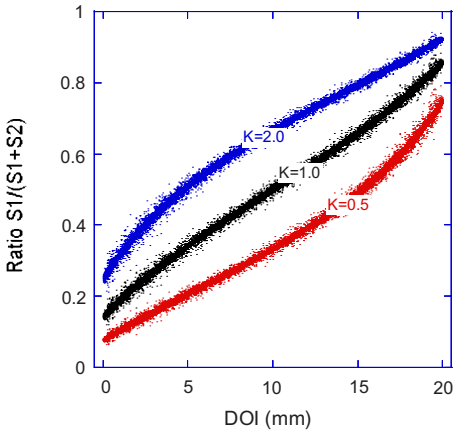

FIG. 9. Similar signal ratio as a function of DOI position as shown in Fig. 6, but the signals were further dispersed with an 18% energy resolution based on the algorithm defined in Eq. (10).

ciple also uniform if the detector is irradiated with a uniform source and the effect of gamma ray escaping at crystal edge is small.

(3) There is no assumption or approximation of any particular relationship between the detector response and DOI positions since Eq. (5) and (6) is valid for any PDF(R). Therefore, the new method significantly simplifies the data processing and consequently improves the accuracy in determining DOI function by avoiding any approximation or assumption of detector response functions, and can be in theory applied as a general method to any detector performance under different operating conditions.

(4) DOI function is measured continuously from one crystal end to the other, which accelerates the data processing with a simple integration. More importantly, a continuous DOI function will permit DOI to be calculated straightforwardly for any values of signal ratios, an advantage to avoid any potential error from binning effects.

To quantitatively understand the accuracy of the new method under various conditions that can significantly affect DOI measurement, such as impact of gamma ray scatters and energy depositions, different gamma interactions for crystals at the surface or inside the array, and limited energy resolutions of a realistic detector, etc., Monte Carlo simulations and experimental measurements have been conducted and are illustrated in the following.

II.C. Monte Carlo simulation studies

GATE (GEANT4 application for tomographic emission) simulation software was used to simulate gamma interactions with a practical detector configuration.[24] As shown in Fig. 3, the detector consists of an 8×8 array of $2\times2\times20$ mm^3 LSO crystals. Each crystal is optically isolated from the others, and measured by photon sensors from its two ends. Since a point source at a distance is usually used in practice to mimic a uniform irradiation source, a point source was placed 30 cm away in the simulation from the side of the crystal array and at the line that is perpendicular to the side and across the center of the crystal array. With this setup, an approximate parallel beam of gamma rays was simulated as a uniform irradiation source to the array, with a $\sim2°$ maximum spreading angle from the ideal parallel beam. All interaction positions and deposited energies were recorded, including intercrystal scatters among different crystals.

For the sake of simplicity, the crystals that were exposed directly to the gamma ray beam are defined as the *front* crystals; the rest of the crystals are defined as the *back* crystals. In general, the front crystals were irradiated with mostly 511 keV gamma rays and a small fraction of backscatters, while the back crystals could have significantly more intercrystal scatters with less than 511 keV energies. As an example, the distributions of simulated DOI positions for the front and back crystals with different energy thresholds are shown in Fig. 4. The results indicate that DOI positions with a 350–650 keV energy window are uniformly distributed across the crystal length for all crystals, except drops at the

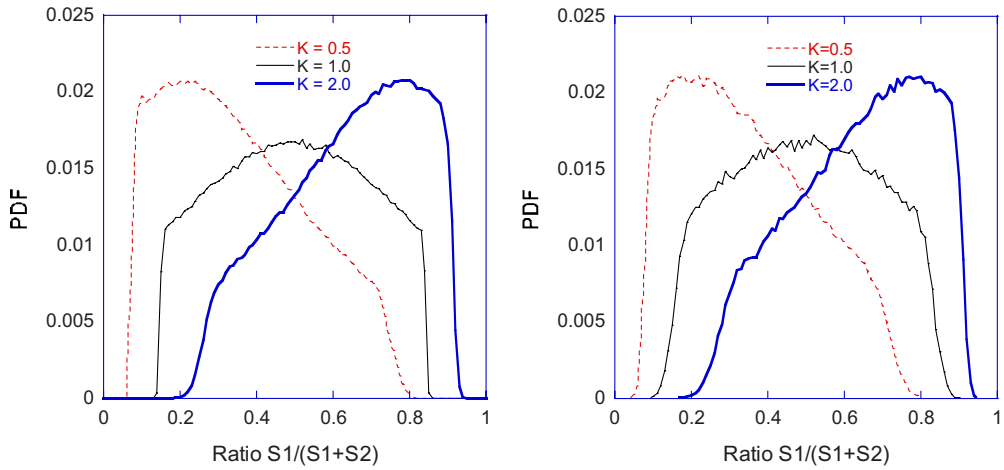

FIG. 10. Calculated PDFs with signal dispersion, with energy thresholds at 200–650 keV (left) and 350–650 keV (right).

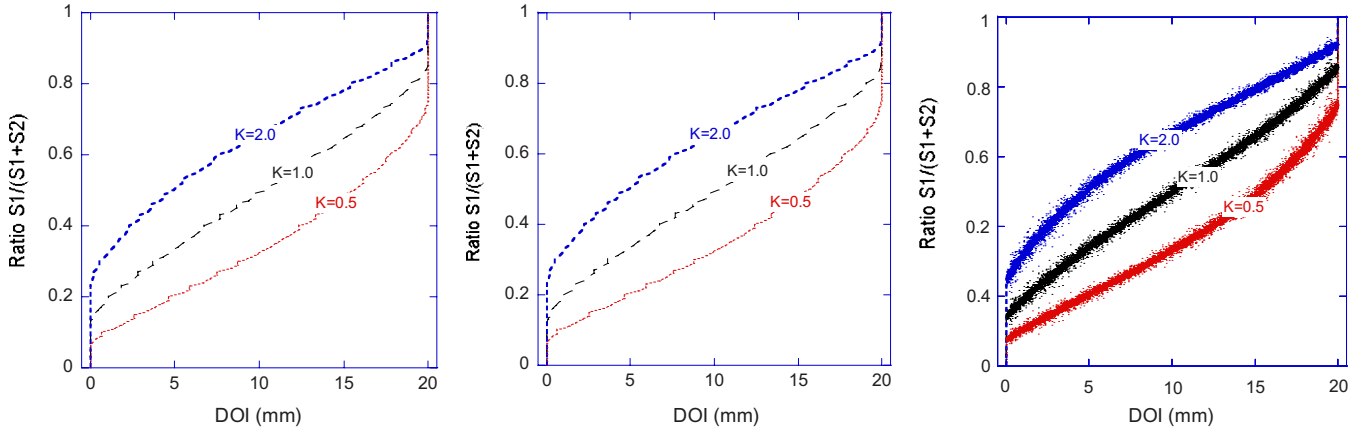

FIG. 11. Calculated DOI functions with signal dispersion, with energy thresholds at 200–650 keV (left) and 350–650 keV (middle). Both DOI functions were superimposed together with dispersed original DOI function (right).

very ends due to the gamma ray escaping at the scintillator edges. DOI positions with a 200–650 keV energy window are slightly less uniformly distributed with the back crystals. This is because lower-energy scatters tend to spread to a larger region and consequently there are more gamma ray escaping at the crystal edges. Simulations with both energy windows were carried out for the calculation of DOI functions.

The signals of each crystal were processed individually, assuming that there was no signal crosstalk or multiplexing among different crystals. For two photon sensors, their light collections are defined as $f_1(z')$ and $f_2(z')$, where z' is the normalized DOI. In general, these light functions are monotonic functions of z'. The amplification gains (usually combined with their readout electronics) of the photon sensors are defined as g_1 and g_2, with $k=g_1/g_2$. According to Eq. (2), the ratio of signals will be

$$R=\frac{g_1*f_1(z')}{g_1*f_1(z')+g_2*f_2(z')}=\frac{k*f_1(z')}{k*f_1(z')+f_2(z')}. \tag{7}$$

Instead of using a photon propagation simulation that depends on the specific crystal surface conditions,[25] which demands complex processing and long calculation time, the sine functions were modeled as the scintillation light collection functions of the photon sensors, which in general provides a basis to study the relationship between DOI function measurement and the realistic signal detection and processing.[20,22,23] These functions are defined as

$$f_1(z')=\sin\left(\frac{\pi}{2}z'\right)+b, \tag{8}$$

$$f_2(z')=\sin\left(\frac{\pi}{2}(1-z')\right)+b, \tag{9}$$

where b is a constant baseline value to model the nonzero value of light collection at the crystal edges. For this simulation, b is chosen to be 0.2. The k values are chosen to be 0.5, 1.0, and 2.0 respectively to represent reasonable range of different gain ratios between the two photon sensors under normal operating conditions, and there should be an inverse relationship between the calculations with $k=0.5$ or 2.0.

The signal dispersion related to the detector energy resolution was also modeled: The signal amplitude S_0, which was originally calculated from Eqs. (8) and (9), was blurred according to a Gaussian function, with S_0 as the mean and the following as the standard deviation:

$$\sigma=\frac{S_0}{2.355}\left(\frac{\Delta E}{E}\right), \tag{10}$$

where $(\Delta E/E)$ is the detector energy resolution, which is usually a complicated function of DOI positions and signal amplitudes. To simplify the problem, a constant value of energy resolution (18%) over different DOI positions was used as a first-order approximation to blur the signals.

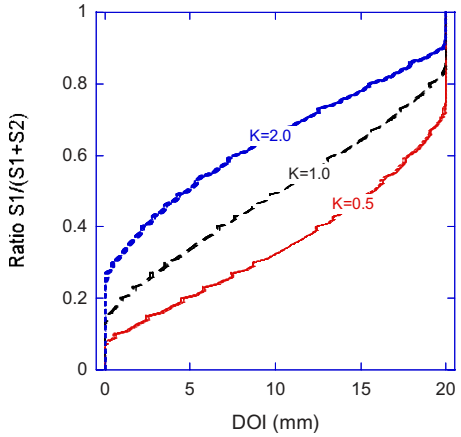

FIG. 12. Total 36 DOI functions calculated from combinations of energy thresholds (200–650 and 350–650 keV), signal dispersions (with and without), K values (0.5, 1.0, and 2.0), and crystal locations (one front and two back crystals, or f_2, m_2, and r_2 defined in Fig. 3). The differences among the functions with the same K value are negligibly small.

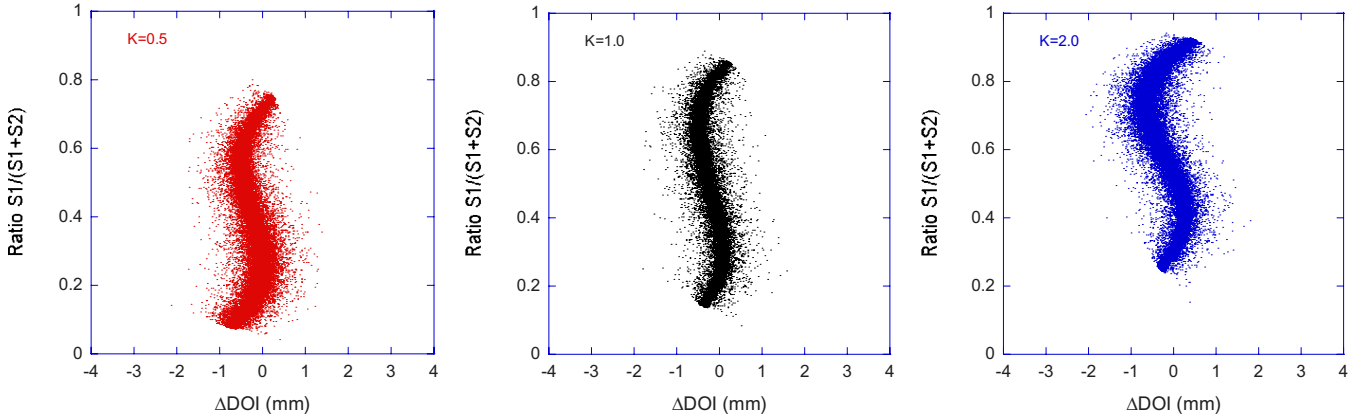

FIG. 13. Distributions of DOI calculation errors with different K values based on the calculation of a back crystal. From left to right, $K=0.5$, 1.0, and 2.0. Most errors are less than 1.0 mm.

II.D. Experiment validation

The setup for DOI function measurement is very similar to the one shown in Fig. 1, which has been used previously by several groups.[8,14,18,19] A $1.8\times2\times20$ mm^3 LSO crystal was connected to two single-channel PMTs (Hamamatsu R7400-02) at its two ends. Since the purpose of this experimental study is to evaluate the new method for DOI function measurement and its accuracy, PMTs were used to take advantage of their simple setup and good performance stability compared to semiconductor photon sensors. The signal amplitudes, S_1 and S_2, from these two PMTs were measured, and the ratio of the signals, $R=S_1/(S_1+S_2)$, was recorded as a function of DOI position.

DOI function was first measured with the primary current method: A second detector, which consisted of a $2\times2\times10$ mm^3 LSO crystal coupled to a single-channel photon sensor (Photonique SSPM-0409), was used to determine DOI positions with an electronic collimation. A Na-22 point source (~1.0 mm diameter) and the second detector were stepped over the first detector along its long crystal axial direction. The step size was 2.0 mm. Signals from both PMTs at each DOI position were acquired and summed with equal signal gains. A 300 keV low energy threshold for summed signal was used during acquisitions. The ratio of the signals R was calculated and DOI function was measured as $R(z)$. The accuracy of DOI localization in the first detector by the electronic collimation method can be estimated from the geometry of the source and detector positions. With a source diameter ~1.0 mm and the distances between the source and the first and second detectors being equal to ~60.0 mm, the uncertainty of DOI localization was estimated to be ~1.4 mm.

DOI function was also measured with the new method without the use of the second detector. The Na-22 point source was placed ~21.3 cm away from the crystal, which provided gamma rays that irradiated the first detector with a ~2.7° maximum angle deviating from the parallel beams. To measure DOI functions of the back crystals, a simple setup was used to mimic the similar impact of intercrystal scatters: A bulk of LSO scintillator with 30.0 mm thickness was placed between the first LSO crystal and the point source (Fig. 5), while all measurement conditions were kept the same. Therefore, without or with the use of this bulky crystal, DOI functions can be easily measured and compared in the situation with the front or back crystals in a crystal array. It is expected that DOI functions measured from both experiments should be the same, since the operating conditions of the first detector had been kept the same during the two measurements.

III. RESULTS

III.A. The results of Monte Carlo simulation studies

To quantitatively understand the effectiveness and accuracy of the new method, signals from some exemplified front and back crystals were calculated from the raw data of simulated gamma interactions and were used to calculate various distributions and DOI functions, either without or with signal dispersions.

The relationship between the original DOI positions with respect to the corresponding signal ratios without any signal dispersion is shown in Fig. 6, which was calculated from a

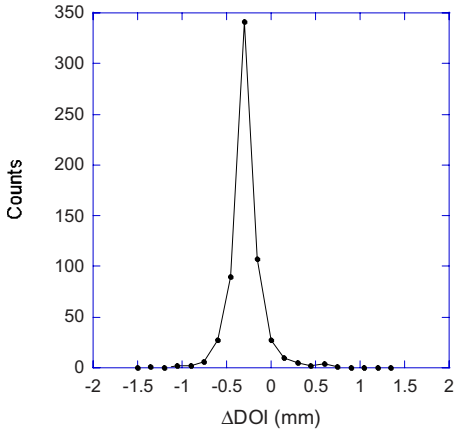

FIG. 14. A profile that corresponds to the projection horizontally across DOI error distribution shown in Fig. 13 with $K=1.0$ and signal ratios $=0.5\pm0.01$.

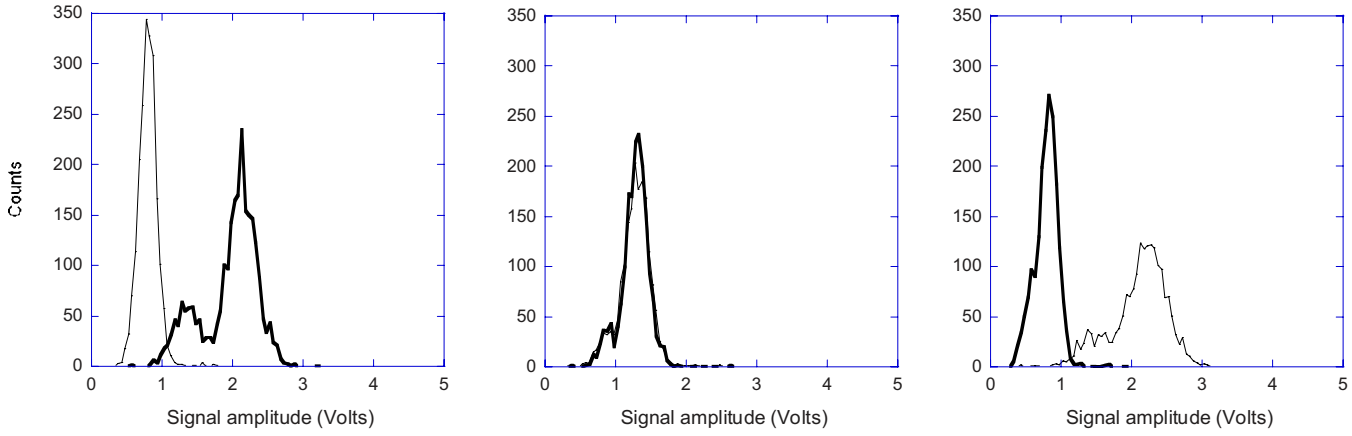

FIG. 15. Energy spectra measured from both PMTs at different DOI positions. From left to right, DOI=0.0, 10.0, and 20.0 mm.

typical front crystal with different K values equal to 0.5, 1.0, and 2.0. It is clear that there is a unique one-to-one correspondence between a DOI position and a signal ratio. Distributions of PDF functions with different energy thresholds were calculated and shown in Fig. 7, and the calculated DOI functions with the new method are shown in Fig. 8. The differences between these functions with the same K values are small, indicating that the overall distribution of signal ratios is not sensitive to slightly nonuniformity of distribution of original DOI positions.

When the energy resolution is not perfect, the relationships between the original DOI positions and the signal ratios are no longer unique, and interactions at the same DOI position will have different signal ratios due to the signal dispersion. The same data shown in Fig. 6 were reprocessed with signal dispersion corresponding to an 18% energy resolution and shown in Fig. 9. Distributions of typical PDF functions at different energy thresholds were recalculated and shown in Fig. 10. DOI functions were recalculated as well and shown in Fig. 11. The differences between the functions with the same K values are also small, indicating that the overall distribution of signal ratios may not be sensitive to different energy thresholds, although this remains to be further studied with more realistic simulation based on light photon tracking.

However, as shown in Fig. 11, the differences among DOI functions with different K values are distinctively large, indicating that DOI function is sensitive to the gain variations between the two photon sensors in the DES readout, and it is necessary to recalibrate DOI function when the detector gain changes.

Similar calculations were applied to the back crystals as well. In Fig. 12, DOI functions calculated with different energy thresholds and resolutions from two different back crystals that were selected from the middle and faraway rear side of the detector array were superimposed with the ones calculated from the front crystal. They were calculated with and without energy dispersions. The differences among the 12 different DOI functions with the same K values are very small so that they can be practically considered to be identical, which indicates that the new method provides a robust DOI function measurement for different energy resolutions, thresholds, and crystal locations inside the detector array. This is mainly attributed from the fact that the new method is strongly correlated to the average detector response to DOI, which is calculated from the integration of different interaction positions over the crystal, as shown in Eq. (5). Therefore, this "long-range" property of signal contribution alleviates the variations from various factors.

The error between the calculated and original DOI positions was also studied. DOI positions were calculated with a second dataset generated with a new simulation in order to avoid using the same dataset that was used for generating DOI functions. From an original DOI position z_o, the signals were dispersed, the signal ratio R_o was calculated and used to obtain the calculated DOI position with the calibrated DOI function, $z_c=z(R_o)$. The error of DOI determination was calculated as $\Delta\text{DOI}=z_c-z_o$. The typical distributions of these errors with different K values are shown in Fig. 13, based on the calculation from a back crystal. A typical profile of DOI error distribution is shown in Fig. 14. Most DOI calculation errors (more than 99%) are less than 1.0 mm.

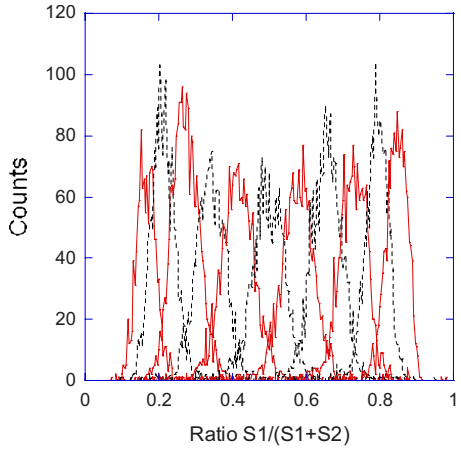

FIG. 16. Distributions of signal ratios calculated from data acquired at different DOI positions, ranging from 0.0 to 20.0 mm and with a 2.0 mm step size. Different line legends were used only for better readability.

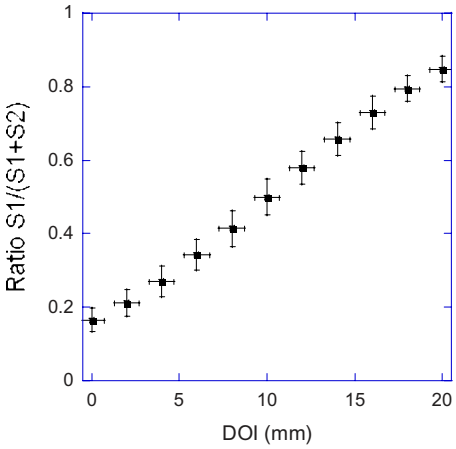

FIG. 17. DOI function measured from the primary current method.

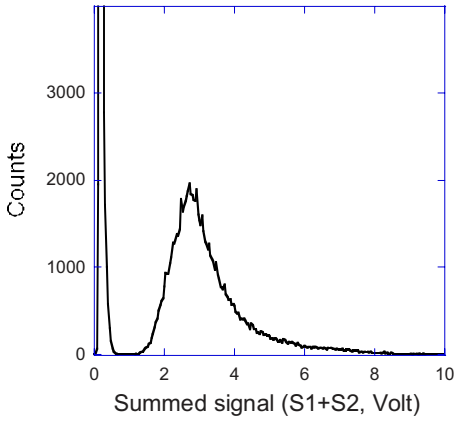

FIG. 19. Energy spectrum measured from the summed signals of two PMTs with accumulated interactions from all different DOI positions.

III.B. The results of experimental measurements

DOI function was initially measured with the primary current method as the basis to compare with the new method. Some typical signal spectra acquired from both PMTs are shown in Fig. 15. Note the substantial shift of signal amplitudes with respect to different DOI positions, which reflects the capability to measure DOI. The distribution of the signal ratios, S1/(S1+S2), calculated on an event-by-event basis, is shown in Fig. 16 for 11 different DOI positions, ranging from 0.0 to 20.0 mm (from right to the left crystal end). The symmetric characteristic of this distribution over the range of signal ratios also suggests that the gains of photon sensors at both crystal ends were about the same for these measurements.

In order to quantitatively calculate DOI function, the mean and FWHM (full-width at half-maximum) of each ratio distribution were calculated with a Gaussian curve fit.[14] The results are shown in Fig. 17, which is DOI function $R(z)$ that provides the quantitative relationship between the signal ratio R and DOI position z. The error bars associated with each DOI position were calculated as the uncertainty of DOI localization (~1.4 mm) and the FWHM of the fitted signal ratio distribution (Fig. 16).

The energy resolutions measured from summed signals are quite uniformly distributed for different DOI positions, as shown in Fig. 18, with an average value of 16.5%, ranging from 15.0% to 19.6%. These results are consistent with the other measurements.[18,19,23,25]

With the same detector operating conditions, DOI function was measured again with the new method. The detector was roughly uniformly irradiated by the point source which was placed ~213.0 mm away from the side of the scintillator array. The spectrum of summed signals is shown in Fig. 19. Since there was no DOI localization and the valid events were acquired from different DOI positions, the energy resolution was relatively poor (~47%). A low signal threshold at 1.0 V was applied to get rid of those spurious events at very low signal levels due to the mistriggering of the data acquisition at the high count rate. The PDF was calculated as a normalized distribution of signal ratios and is shown in Fig. 20, which is also quite symmetric over the range of signal ratios.

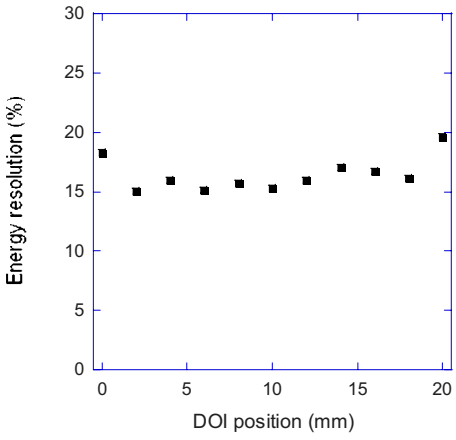

FIG. 18. Energy resolutions measured from the summed signals of two PMT's at different DOI positions.

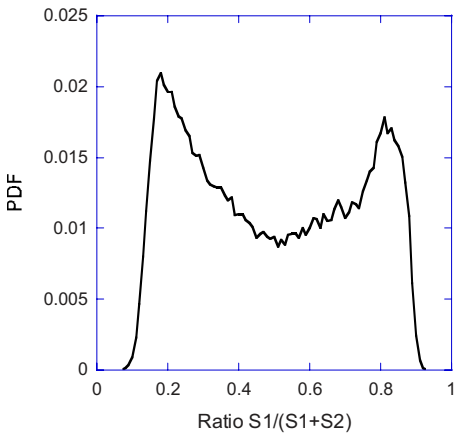

FIG. 20. PDF function calculated from the same measured data shown in Fig. 19, with a minimum threshold at 1.0 V.

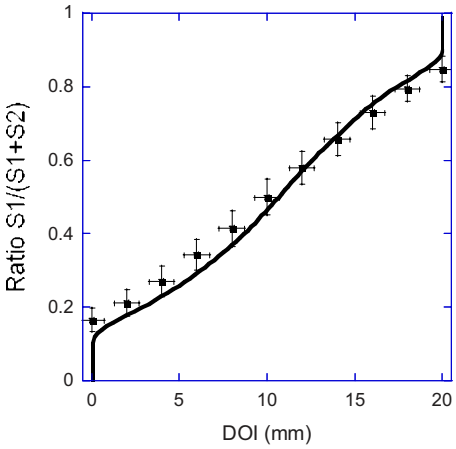

FIG. 21. DOI functions measured with the new method (solid line), superimposed with the results from the current method (dots with error bars) which is the same data as shown in Fig. 17.

DOI function was calculated with a simple integration of the PDF according to Eq. (6). For comparison, DOI functions measured with the current and new methods are shown in Fig. 21. The two functions are basically overlapped within the error bars; the maximum difference between the two DOI functions is ~1.4 mm. These results show that DOI functions measured from the first current method and the new method are overall in a good agreement, while the latter does not rely on the requirements of complicated DOI localization and the accurate detector-source alignment that can potentially make the measurement significantly difficult and erroneous.

In a separate study, DOI functions were measured with or without intercrystal scatters by placing or removing the bulk LSO crystal between the source and the detector but keeping the same detector operating conditions for the both measurements. Signal spectra of summed signals from both measurements are shown in Fig. 22. Although total acquired counts were different for the two measurements, the corresponding

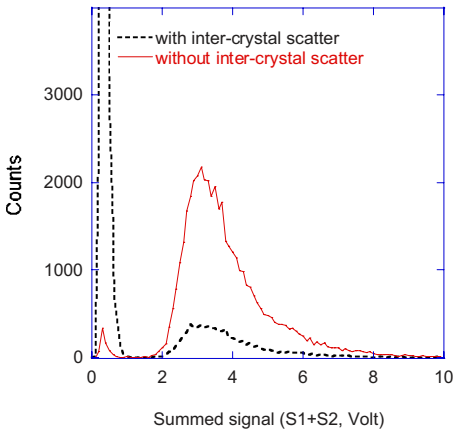

FIG. 22. Energy spectra measured from the summed signals of two PMTs with accumulated interactions from all different DOI positions. The solid and dashed curves correspond to the measurement without and with the intercrystal scatters and attenuation caused by the bulk of LSO scintillator being placed between the source and the detector.

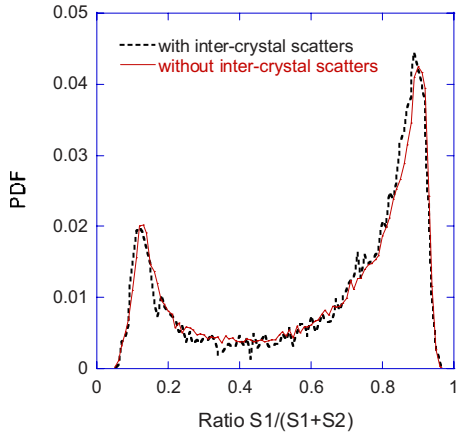

FIG. 23. PDF functions measured from the same acquired data as shown in Fig. 22, with a minimum threshold at 1.0 V. The solid and dashed curves correspond to the measurements without and with intercrystal scatters and attenuation. The two functions are about the same but not symmetric over the range of signal ratios, because the gains of photon sensors at the crystal ends were not the same during these two measurements.

PDF functions are about the same as expected, as shown in Fig. 23, which indicates that the detector had the same signal responses for the measurements either with or without the intercrystal scatter and attenuation. DOI functions calculated from both measurements are shown in Fig. 24. The difference between the two functions is negligibly small; the maximum difference between the two DOI functions is ~0.6 mm. It should be pointed out that although the detector operating conditions were kept the same during these two measurements, they were different from those in the previous studies associated with Figs. 19–21. Therefore, it is expected that the measured PDF and DOI functions are different from the previous ones.

IV. DISCUSSION AND SUMMARY

Although the validations of the new method were based on the use of uniform distribution of gamma interactions (DOI), which is similar to one of the current methods,[22] the

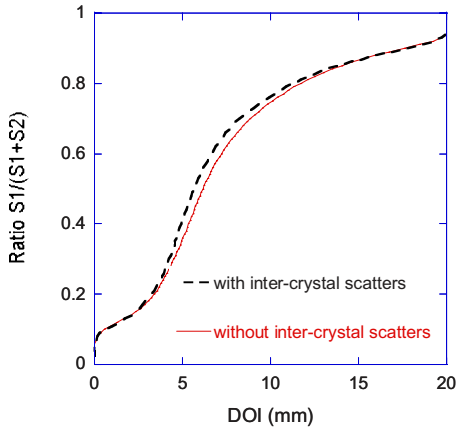

FIG. 24. DOI functions measured with the new method, either without or with intercrystal scatters and attenuation, corresponding to the solid and dashed curves, respectively.

principle and data processing of the two methods are completely different, as illustrated in Sec. II. In addition, in theory, any known distribution of DOI positions can be used to calculate DOI function with the new method [Eq. (4)]. Nevertheless, in practice, a uniform DOI distribution will lead to a much simpler acquisition setup and data processing.

One technical challenge for the new method is that when the detectors are assembled inside a PET system, it is difficult to implement radiation sources with parallel beams to achieve uniform DOI distributions for all detectors. There are two possible solutions to this problem:

(1) As part of the detector evaluation, all detectors will be first calibrated with DOI functions, $z_1(R)$, with the new method described above before they will be assembled. Once all detectors are inside the system, projection data from an external source or phantom that is being placed inside the system gantry will be acquired and processed with the same method as before to have another DOI function, $z_2(R)$. Since the distribution of DOI positions in the second measurement is not uniform anymore, there will be expected discrepancies between the two DOI functions, but with a unique corresponding relationship between the first and second measurements. Therefore, $z_1(R)$ and $z_2(R)$ can be transformed from one to another, and these two are different versions of DOI functions under different source conditions, and both can be used to calculate DOI position of an event from either source with a proper transformation. The future recalibration of DOI function can be based on the $z_2(R)$ with the same principle, once the same setup of external source that was used in measuring the $z_2(R)$ will be kept.
(2) For some scintillator materials with their natural radiation background, such as LSO, the new method can provide a very straightforward DOI function measurement without the use of any external source, if the distribution of internal interaction position is known. The approach will require longer acquisition time and deal with interactions that may have different spectrum characteristics from those induced by external radiations. This study will be reported separately.

In practice, there are other challenges that may complicate the conditions for implementing the new method, such as the cross-talk (optically or electrically) among different crystals, Compton scatter over different crystals, and the change of crystal map with different DOI positions. These effects need to be further investigated as part of the overall detector design, calibration, and optimization.

In summary, a new calibration method to measure DOI function has been developed and validated with Monte Carlo simulations and experimental studies. Compared to the current methods, the new method significantly simplifies the setup and procedure, provides consistent DOI function for very different detector configurations and operating conditions without the need of knowing or assuming detector responses, and enables the calibration of DOI function for all crystals inside a detector array by a single data acquisition. This new method is expected to provide an adequate solution to measure and recalibrate DOI functions of a PET detector that is capable of independent crystal readout and uses the design of DES readout.

[a]Address for correspondence: Department of Imaging Physics, University of Texas M.D. Anderson Cancer Center, 8014A El Rio, Houston, Texas 77054. Electronic mail: yiping.shao@di.mdacc.tmc.edu

[1]S. R. Cherry, J. A. Sorenson, and M. E. Phelps, *Physics in Nuclear Medicine*, 3rd ed. (Saunders, Philadelphia, 2003).
[2]Y. C. Tai and R. Laforest, "Instrumentation aspects of animal PET," Annu. Rev. Biomed. Eng. **7**, 255–285 (2005).
[3]C. S. Levin and H. Zaidi, "Current trends in preclinical PET system design," PET Clin. **2**, 125–160 (2007).
[4]A. F. Chatziioannou *et al.*, "Performance evaluation of microPET: A high-resolution lutetium oxyorthosilicate PET scanner for animal imaging," J. Nucl. Med. **40**, 1164–1175 (1999).
[5]W.-H. Wong, "Designing a stratified detection system for PET cameras," IEEE Trans. Nucl. Sci. **33**(1), 591–596 (1986).
[6]K. Shimizu *et al.*, "Development of 3-D detector system for positron CT," IEEE Trans. Nucl. Sci. **35**(1), 717–720 (1988).
[7]C. Carrier *et al.*, "Design of a high resolution positron emission tomograph using solid state scintillation detectors," IEEE Trans. Nucl. Sci. **35**(1), 685–690 (1988).
[8]W. W. Moses, and S. E. Derenzo, "Design studies for a PET detector module using a PIN photodiode to measure depth of interaction," IEEE Trans. Nucl. Sci. **41**(4), 1441–1445 (1994).
[9]P. Bartzakos and C. J. Thompson, "A depth-encoded PET detector," IEEE Trans. Nucl. Sci. **38**(2), 732–738 (1991).
[10]R. S. Miyaoka *et al.*, "Design of a depth of interaction (DOI) PET detector module," IEEE Trans. Nucl. Sci. **45**(3), 1069–1073 (1998).
[11]S. Yamamoto, and H. Ishibashi, "A GSO depth of interaction detector for PET," IEEE Trans. Nucl. Sci. **45**(3), 1078–1082 (1998).
[12]L. R. MacDonald and M. Dahlbom, "Depth of interaction for PET using segmented crystals," IEEE Trans. Nucl. Sci. **45**(4), 2144–2148 (1998).
[13]H. Murayama *et al.*, "Depth encoding multicrystal detectors for PET," IEEE Trans. Nucl. Sci. **45**(3), 1152–1157 (1998).
[14]Y. Shao *et al.*, "Design studies of a high resolution PET detector using APD arrays," IEEE Trans. Nucl. Sci. **47**(3), 1051–1057 (2000).
[15]P. Bruyndonckx *et al.*, "Neural network-based position estimators for PET detectors using monolithic LSO blocks," IEEE Trans. Nucl. Sci. **51**(5), 2520–2525 (2004).
[16]N. Inadama *et al.*, "Performance of 256ch flat panel PS-PMT with small crystals for a DOI PET detector," IEEE Trans. Nucl. Sci. **52**(1), 15–20 (2005).
[17]J. Seidel, J. J. Vaquero, and M. V. Green, "Resolution uniformity and sensitivity of the NIH ATLAS small animal PET scanner: Comparison to simulated LSO scanners without depth-of-interaction capability," IEEE Trans. Nucl. Sci. **50**(5), 1347–1350 (2003).
[18]K. C. Burr *et al.*, "Evaluation of a prototype small-animal PET detector with depth-of-interaction encoding," IEEE Trans. Nucl. Sci. **51**(4), 1791–1798 (2004).
[19]Y. Yang *et al.*, "Depth of interaction resolution measurements for a high resolution PET detector using position sensitive avalanche photodiodes," Phys. Med. Biol. **51**, 2131–2142 (2006).
[20]W. W. Moses *et al.*, "A room temperature LSO/PIN photodiode PET detector module that measures depth of interaction," IEEE Trans. Nucl. Sci. **42**(4), 1085–1089 (1995).
[21]J. S. Huber, W. W. Moses, and P. R. G. Virador, "Calibration of a PET detector module that measures depth of interaction," IEEE Trans. Nucl. Sci. **45**(3), 1268–1272 (1998).
[22]G. C. Wang *et al.*, "Calibration of a PEM detector with depth of interaction measurement," IEEE Trans. Nucl. Sci. **51**(3), 775–781 (2004).
[23]Y. Shao, H. Li, and K. Gao, "Initial experimental studies of using solid-state photomultiplier for PET applications," Nucl. Instrum. Methods Phys. Res. A **580**, 944–950 (2007).
[24]S. Jan *et al.*, "GATE: A simulation toolkit for PET and SPECT," Phys. Med. Biol. **49**, 4543–4561 (2004).
[25]Y. Shao *et al.*, "Dual APD array readout of LSO crystals: Optimization of crystal surface treatment," IEEE Trans. Nucl. Sci. **49**(3), 649–654 (2002).